Physica E 41 (2009) 1611–1615

Contents lists available at ScienceDirect

Physica E

journal homepage: www.elsevier.com/locate/physe

Fano–Kondo spin filter

A.C. Seridonio [a,b], F.M. Souza [a,c], J. Del Nero [d,e], I.A. Shelykh [a,f,*]

[a] International Center for Condensed Matter Physics, Universidade de Brasília, 70904-970 Brasília, DF, Brazil
[b] Instituto de Física, Universidade Federal Fluminense, 24310-346 Niterói, RJ, Brazil
[c] Instituto de Física, Universidade Federal de Uberlândia, 38400-902 Uberlândia, MG, Brazil
[d] Departamento de Física, Universidade Federal do Pará, 66075-110 Belém, PA, Brazil
[e] Instituto de Física, Universidade Federal do Rio de Janeiro, 21941-972 Rio de Janeiro, RJ, Brazil
[f] Science Department, University of Iceland, Dunhaga 3, IS-107 Reykjavik, Iceland

ARTICLE INFO

Article history:
Received 2 April 2009
Received in revised form
8 May 2009
Accepted 11 May 2009
Available online 19 May 2009

PACS:
72.15.Qm
73.23.−b
85.35.Ds
85.75.−d
07.79.Cz

Keywords:
Kondo effect
Transport
Spintronics
Scanning tunneling microscope
Fano

ABSTRACT

The spin-dependent scanning tunneling spectrum generated by a ferromagnetic tip on a metallic host with a Kondo adatom is discussed. The combined effects of the Kondo screening, quantum interference, and tip magnetism are studied. For short tip–adatom separations, the askew lineshape characteristic of quantum interference in Kondo systems is split into two spin components. For the majority-spin component, the Fano antiresonance is strongly enhanced. With the tip atop the adatom, a window of bias voltages is found in which the tunneling current is nearly 100% spin polarized. In the vicinity of a Kondo adatom, the ferromagnetic scanning tunneling microscope constitutes a powerful spin polarizer.

1. Introduction

The Kondo effect is one of the most fascinating manifestations of strong correlations in electronic systems [1]. First observed as an enhancement of the resistance of dilute magnetic alloys below a characteristic temperature T_K, the effect found a more controlled environment in the early 1990s, following the development of nanoscale miniaturization techniques. Kondo effects in quantum dots (QDs) and QD arrays coupled to metallic or semiconductor electrodes were reported [2]. A variety of mesoscopic phenomena associated with the narrow resonance in the density of states of a QD coupled to conduction-electron reservoirs were reported [3–5]. In particular, the Kondo resonance was shown to an enhance the conductance at low temperatures ($T<T_K$).

The mismatch between the electrode Fermi levels resulting from the application of an external bias splits the Kondo peak into two resonances [6–13]. If the electrodes are ferromagnetic, the large local exchange field splits further the resonances. The separation between the peaks now depends on the relative directions of the electrode magnetizations, and on the external magnetic field [14–18]. Current technology allows the construction of single QD devices and routine observation of all such phenomena [19,20].

In an alternative nanoscale setup, a magnetic atom is adsorbed on a metallic host and probed by a scanning tunneling microscope (STM) tip, either normal or ferromagnetic. The quantum interference between currents flowing from the tip to the host directly or by the way of the adatom gives rise to a rich variety of transport regimes. In particular, at temperatures below T_K, in analogy with the distortion of a Lorentzian into an antiresonance in conventional Fano systems [21], the interference distorts the contribution of the Kondo resonance to the adatom spectral function. Antiresonances with such characteristics have been widely reported in experiments with nonmagnetic tips [22–26] and discussed theoretically [27–30].

The development of FM tips [31] makes adatom systems potentially important actors in the rapidly developing field of spintronics [32]. Recently, following a report by Patton et al. of a theoretical study of the conductance for a ferromagnetic tip in the

* Corresponding author at: Instituto de Física, Universidade Federal de Uberlândia, 38400-902 Uberlândia, MG, Brazil.
E-mail address: fmsouza@infis.ufu.br (F.M. Souza).

1386-9477/$ - see front matter
doi:10.1016/j.physe.2009.05.006

Kondo regime [33], the present authors investigated the dependence of the conductance on the tip–adatom separation in a full range of the Fano parameters, defined as the ratio between tip–adatom and tip–host couplings [34].

Here, we analyze a spin-resolved conductance for FM tip–adatom–host metal system in the weak-coupling regime, in which tunneling amplitudes can be treated as perturbations. To account for the Kondo effect, we refer to the Doniach–Sunjic-like expression for the adatom spectral function [35–38]. We find that very weakly magnetized tips can generate strongly spin-polarized currents [39,40]. For certain configurations, in an appropriate bias interval, the current can be fully spin-polarized, an effect due to the suppression of one spin component by the spin splitting of the Fano–Kondo resonance. The influence of the tip–adatom separation on this *spin-polarizing device* is also investigated.

2. Theoretical model

We consider the following model Hamiltonian:

$$\mathscr{H} = \mathscr{H}_{SIAM} + \mathscr{H}_{tip} + \mathscr{H}_{T}, \tag{1}$$

where ($\mathscr{H}_{tip}$) represents the ferromagnetic tip, the $\mathscr{H}_T$, the host–tip coupling, and ($\mathscr{H}_{SIAM}$) is the spin degenerate Anderson Hamiltonian representing the host and the magnetic impurity coupled to it [41]:

$$\mathscr{H}_{SIAM} = \sum_{\vec{p}\sigma} \varepsilon_{\vec{p}} a^{\dagger}_{\vec{p}\sigma} a_{\vec{p}\sigma} + \varepsilon_0 \sum_{\sigma} c^{\dagger}_{0\sigma} c_{0\sigma} + U n_{0\uparrow} n_{0\downarrow} + v \sum_{\sigma} (f^{\dagger}_{0\sigma} c_{0\sigma} + H.C.), \tag{2}$$

where $a_{\vec{p}\sigma}$ is a fermionic operator for a conduction electron with momentum $\vec{p}$ and spin σ; $c_{0\sigma}$ is a fermionic operator for an electron localized on adatom state; and ε_0 and U are the energy of the adatom level and Coulomb repulsion between two electrons with opposite spins at the adatom site, respectively (Fig. 1).

For simplicity, we consider a structureless conduction band with density of states ρ_0. The half bandwidth is denoted by D. To describe the hybridization between the band and the impurity, we introduced the shorthand

$$f_{0\sigma} = \frac{1}{\sqrt{N}} \sum_{\vec{p}} a_{\vec{p}\sigma}, \tag{3}$$

where N is the number of conduction states.

We focus the Kondo regime, which favors the formation of a localized magnetic moment at the adatom, i.e., the conditions $\varepsilon_0 < \varepsilon_F, \varepsilon_0 + U > \varepsilon_F$ and $\Gamma \ll |\varepsilon_0|,\ \varepsilon_0 + U$. At temperatures $T \ll T_K$, the antiferromagnetic correlations introduced by the coupling to the host electrons screen the impurity moment and add a narrow resonance, of half-width $k_B T_K$, centered at the Fermi level, to the adatom spectral density. The Kondo temperature is approximately given by the expression [42]

$$k_B T_K = \sqrt{\frac{\Gamma U}{2}} \exp[\pi \varepsilon_0 (\varepsilon_0 + U)/2\Gamma U]. \tag{4}$$

We neglect the electron–electron interactions in the FM tip and write

$$\mathscr{H}_{tip} = \sum_{\vec{k}\sigma} (\varepsilon_{\vec{k}} + eV) b^{\dagger}_{\vec{k}\sigma} b_{\vec{k}\sigma}, \tag{5}$$

where the $b_{\vec{k}\sigma}$'s are the tip conduction states and V is the tip bias voltage. For a ferromagnetic tip, the spin-dependent density of states is

$$\rho^{\sigma}_{tip} = \rho_0 (1 + \sigma p), \tag{6}$$

where p is the magnetization. The tip–host–adatom tunneling Hamiltonian reads

$$\mathscr{H}_T = \sum_{\vec{k}\sigma} b^{\dagger}_{\vec{k}\sigma} \left(t \sum_{\vec{p}} \varphi_{\vec{p}}(\vec{R}) a_{\vec{p}\sigma} + t_{0R} c_{0\sigma} \right) + H.C., \tag{7}$$

where t and $t_{0R} = t_0\, e^{-k_F R}$ are the tip–host and tip–adatom hopping amplitudes, respectively. Following Ref. [29], we let t_{0R} decay exponentially with the tip–adatom lateral distance R. The amplitude t depends on the conduction wave function $\varphi_{\vec{p}}(\vec{R})$ at the tip position $\vec{R}$.

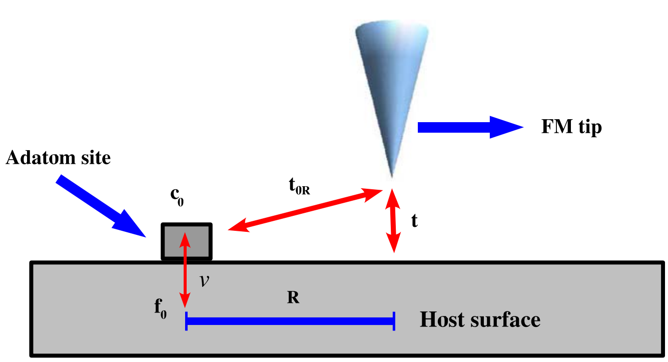

Fig. 1. Scanning tunneling microscope (STM) device with a ferromagnetic (FM) tip with an adsorbed magnetic atom (Kondo adatom) on the surface of a normal metal (host surface). In the host surface, the adatom site (c_0) is hybridized with the metal conduction band (f_0) through the hopping v. The interference between the hopping elements t_{0R} and t leads to the Fano–Kondo profile in the conductance.

3. The conductance formula

To derive an expression for the conductance, we treat the tunneling Hamiltonian (7) to linear order in perturbation theory [27–30] under typical experimental conditions $eV \ll D$. The low-temperature conductance is then

$$G(eV, T \ll T_K, R) = \sum_{\sigma} G_0 \left[\frac{\rho^{\sigma}_{tip}}{\rho_0}\right] \left[\frac{\rho^{\sigma}_{0R}}{\rho_0}\right], \tag{8}$$

where

$$G_0 = (2\pi t \rho_0)^2 \left(\frac{e^2}{h}\right) \tag{9}$$

is the background conductance and

$$\rho^{\sigma}_{0R}(eV) = \rho_0 \left\{ 1 - \left(\frac{\mathscr{F}_{k_F R}}{\rho_0}\right)^2 + \frac{\tilde{\rho}^{\sigma}_{0R}(eV)}{\rho_0} \right\} \tag{10}$$

is the density of states of the host–adatom–tip system. The function

$$\mathscr{F}_{k_F R} = \sum_{\vec{k}} \varphi_{\vec{k}}(\vec{R}) \delta(\varepsilon_k - \varepsilon_F) = \rho_0 J_0(k_F R), \tag{11}$$

where J_0 is the Bessel function of order zero, accounts for the dependence of the conductance on the tip–adatom separation $\vec{R}$. The last term within curly brackets on the right-hand side of Eq. (10) is

$$\tilde{\rho}^{\sigma}_{0R}(eV) = \sum_{m} |\langle m| \left(\frac{\mathscr{F}_{k_F R}}{\rho_0}\right) f_{0\sigma} + \pi \rho_0 v q_R c_{0\sigma} |\Omega\rangle|^2 \times \delta(E_m - E_{\Omega} - eV), \tag{12}$$

where $|\Omega\rangle$ ($|m\rangle$) is the ground state (an eigenstate) of the Anderson Hamiltonian (2). To highlight the interference between the tunneling paths t_{0R} and t built in Eq. (10), we have defined the Fano parameter [29]

$$q_R = (\pi\rho_0 v)^{-1}\left(\frac{t_{0R}}{t}\right) = q_{R=0}e^{-k_F R}. \tag{13}$$

With $q_R \gg 1$ ($q_R \ll 1$) the tip–adatom (tip–host) current is dominant. With $q_R \approx 1$, the current results from a competition between the two conduction paths. As explained in detail in Ref. [34], Eq. (10) can be rewritten as

$$\rho^{\sigma}_{0R}(eV) = \rho_0\left\{1 - \left[\left(\frac{\mathscr{F}_{k_F R}}{\rho_0}\right)^2 - (\tilde{q}_R)^2\right]\times\pi\Gamma\rho^{\sigma}_{ad}(eV) + 2\Gamma\left(\frac{\mathscr{F}_{k_F R}}{\rho_0}\right)\tilde{q}_R\Re\{G^{Ret}_{ad\sigma}(eV)\}\right\}, \tag{14}$$

where

$$\tilde{q}_R = q_R + \left(\frac{\mathscr{F}_{k_F R}}{\rho_0}\right)q \tag{15}$$

is an effective Fano parameter,

$$q = \frac{\sum_{\vec{k}}\dfrac{1}{eV - \varepsilon_{\vec{k}}}}{\pi\rho_0} = \frac{1}{\pi}\ln\left|\frac{eV + D}{eV - D}\right| \tag{16}$$

is the Fano parameter for the Anderson Hamiltonian (2) decoupled from the tip [27–30] and

$$\begin{aligned}\rho^{\sigma}_{ad}(eV) &= -\frac{1}{\pi}\Im\{G^{Ret}_{ad\sigma}(eV)\}\\ &= \frac{1}{\pi\Gamma}\Re\left[\frac{i\Gamma_K}{(eV + \sigma\delta) + i\Gamma_K}\right]^{1/2}\\ &= \frac{1}{\pi\Gamma}\sin^2\delta^{\sigma}_{eV}\end{aligned} \tag{17}$$

is the adatom spectral density, here expressed in three alternative ways: as the imaginary part of the interacting adatom Green's function $G^{Ret}_{ad\sigma}(eV)$; by an analytical Doniach–Sunjic-like expression [35–38]; or by the conduction-state phase shift δ^{σ}_{eV}, respectively.

The ferromagnetic exchange interaction between the tip and the magnetic adatom [14,17] lifts the spin degeneracy of the adatom level ε_0 and hence splits the Kondo resonance into two peaks separated by an energy δ. A "poor man's" scaling analysis [14,33] yields an estimate of δ:

$$\begin{aligned}\delta &= \varepsilon_{0\downarrow} - \varepsilon_{0\uparrow}\\ &= \frac{\gamma^{\uparrow}_{tip} + \gamma^{\downarrow}_{tip}}{2\pi}p\ln(D/U)\\ &= \left[\frac{\gamma_{tip}}{\pi}\ln(D/U)\right]p\exp(-2k_F R),\end{aligned} \tag{18}$$

where

$$\begin{aligned}\gamma^{\sigma}_{tip} &= \pi\rho^{\sigma}_{tip}|t_{0R}|^2\\ &= \gamma_{tip}(1 + \sigma p)\exp(-2k_F R).\end{aligned} \tag{19}$$

Since $eV \ll D$, the right-hand side of Eq. (16) is very small, which shows that it is safe to neglect the last term on the right-hand side of Eq. (15). The spin-resolved conductance is therefore

$$G^{\sigma}/G_{max} = \left[\frac{\rho^{\sigma}_{tip}}{\rho_0}\right]\left[\frac{\rho^{\sigma}(eV)}{\rho_0}\right], \tag{20}$$

where

$$G_{max} = (1 + q_R^2)G_0 \tag{21}$$

and

$$\rho^{\sigma}(eV) = \rho^{\sigma}_{0R}(eV)/(1 + q_R^2). \tag{22}$$

To simplify Eq. (20), we now let the equivalence $\tan\delta_{q_R} \equiv q_R$ define a Fano-parameter phase shift δ_{q_R} and note that

$$\tan\delta^{\sigma}_{eV} = -\frac{\Im\{G^{Ret}_{ad\sigma}(eV)\}}{\Re\{G^{Ret}_{ad\sigma}(eV)\}}. \tag{23}$$

For $R = 0$ we then find that

$$G^{\sigma}/G_{max} = (1 + \sigma p)\cos^2(\delta^{\sigma}_{eV} - \delta_{q_{R=0}}), \tag{24}$$

which gives access to the spin polarization of the tunneling current:

$$\wp = \frac{G^{\uparrow} - G^{\downarrow}}{G^{\uparrow} + G^{\downarrow}}. \tag{25}$$

4. Results

To illustrate our discussion we have chosen the following set of model parameters: $q_{R=0} = 1$, $\varepsilon_0 = -0.9$ eV, $\gamma_{tip} = \Gamma = 0.2$ eV, $U = 2.9$ eV, $D = 5.5$ eV, $T_K = 50$ K, and $k_F = 0.189\,Å^{-1}$ [28,33]. The Kondo temperature was estimated using Eq. (4).

Fig. 2 shows the spin polarization $\wp$ as a function of the bias voltage for differing tip magnetization parameter p. As expected, $\wp$ vanishes for $p = 0$. For $p \neq 0$, two features of $\wp$ stand out: (i) a plateau $\wp \approx +1$, with p-dependent width, centered at $eV = 0$ and (ii) a narrow dip, which sinks to -1, centered at a negative, p-dependent bias. As p is increased, the plateau broadens, while the dip is shifted toward negative biases. For $p = 1$ (fully polarized tip), again as expected, the spin polarization curve saturates at $\wp = 1$. Remarkably, the 100% polarization plateau persists even at weak tip magnetizations, e.g., $p = 0.2$. For sufficiently high voltages, the spin polarization becomes constant, $\wp = p$.

The tip voltage V controls the spin polarization of the current, which can be tuned from -1 to $+1$. The literature contains a number of proposed spin filters [43–46] and spin diodes [47], a few of which have been constructed in the laboratory [48]; dynamic control of the current polarization by time-dependent bias voltages has also been proposed [49,50]. To the best of our knowledge, however, ours is the first demonstration that the interplay between the Kondo effect and quantum interference can control and amplify the spin polarization of the current.

Fig. 3 shows the spin-resolved conductances $G^{\uparrow}$ and $G^{\downarrow}$. For $p = 0$ we find $G^{\uparrow} = G^{\downarrow}$. The interference between the two tunneling paths accounts for the asymmetric Kondo resonance,

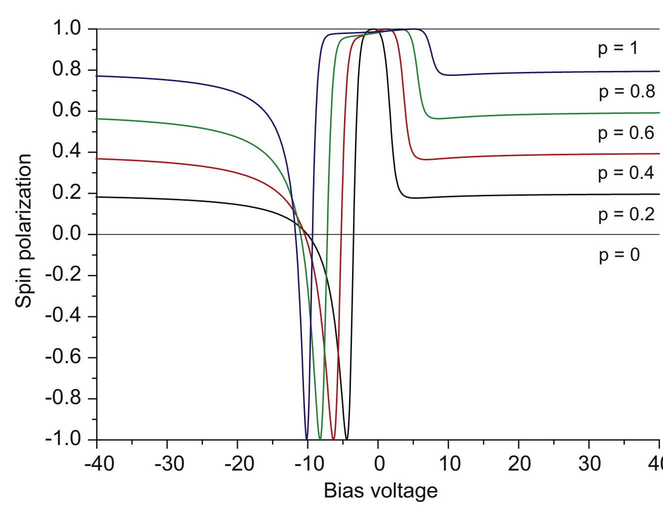

Fig. 2. Spin polarization ($\wp$) at $R = 0$ as a function of the bias voltage eV in units of the Kondo half-width Γ_K for $q_{R=0} = 1$ and tip magnetizations ranging from $p = 0$ to 1. For nonzero p's, $\wp$ reaches a unitary plateau in a magnetic polarization dependent range centered at $eV = 0$. At negative voltages, the spin polarization dips to $\wp = -1$. Following Refs. [28,33], we have set $\varepsilon_0 = -0.9$ eV, $\gamma_{tip} = \Gamma = 0.2$ eV, $U = 2.9$ eV, $D = 5.5$ eV, $T_K = 50$ K, and $k_F = 0.189\,Å^{-1}$.

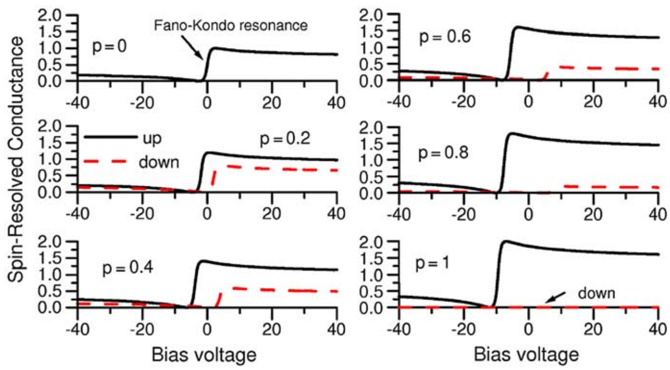

Fig. 3. Spin-resolved conductances (24) for tip atop the adatom ($R=0$), as functions of the bias voltage eV in units of the Kondo half-width Γ_K for $q_{R=0}=1$. For a nonmagnetic tip ($p=0$) the identical spin resolved conductances $G^{\uparrow}$ and $G^{\downarrow}$ display the Fano–Kondo line shape. A ferromagnetic tip ($p \neq 0$) displaces the spin-resolved antiresonances to different energies. A window of energies in which $G^{\downarrow} \approx 0$ while $G^{\uparrow}$ is maximum results. In this region, the spin polarization $\wp$ is unitary. Model parameters as in Fig. 2.

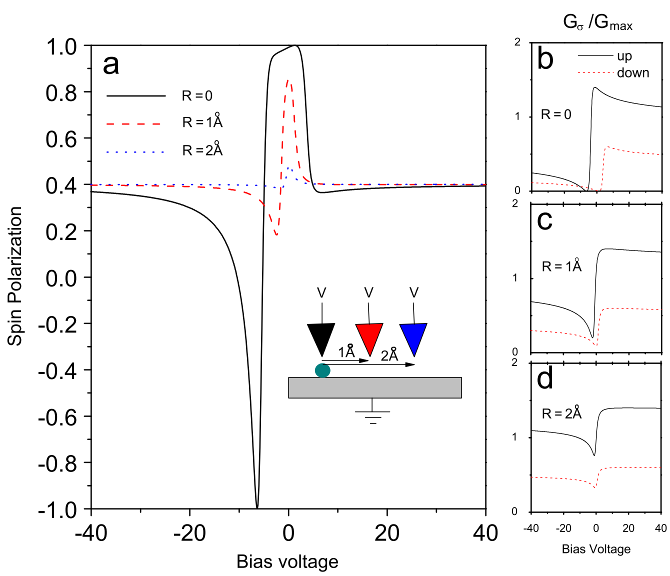

Fig. 4. (a) Spin polarization ($\wp$) as a function of bias voltage eV in units of the Kondo half-width Γ_K for fixed tip magnetization $p=0.4$, $q_{R=0}=1$ and differing tip–adatom lateral displacements R. Large separations R wash out the marked structure of the spin polarization visible at $R=0$, and force the polarization into coincidence with the ferromagnetic polarization p. Panels (b)–(d) show the evolution of the spin resolved conductances, $G^{\uparrow}$ and $G^{\downarrow}$, with the distance. As R increases, the energy splitting between the $G^{\uparrow}$ and $G^{\downarrow}$ antiresonances and the prominence of each antiresonance is reduced. A sketch of the experimental setup appears in the inset. Model parameters as in Fig. 2.

a line shape frequently found with nonmagnetic metallic tips [22–26]. As p grows, the conductances become increasingly distinct: $G^{\uparrow}$ ($G^{\downarrow}$) shifts to the left (right) and opens a window of completely spin polarized conductance with $G^{\downarrow} \approx 0$, which corresponds to the $\wp = 1$ plateau in Fig. 2. The narrow $\wp = -1$ dip in Fig. 2 stems from the vanishing of $G^{\uparrow}$ at a negative voltage in each panel of Fig. 3. As the ferromagnetic polarization p increases, while the amplitude of $G^{\uparrow}$ increases, $G^{\downarrow}$ is suppressed. This contrast is due to the density of states at the tip: for $\sigma = -1$ the prefactor on the right-hand side vanishes as $p \to 1$, which forces $G^{\downarrow} \to 0$.

Finally, Fig. 4 shows the spin polarization $\wp$ as a function of the tip–adatom separation R. For large R, the minimum and the maximum $\wp$ are reduced, the current polarization $\wp$ is governed by the tip polarization p, and the polarization curve becomes flat. To explain the behavior at the polarization at smaller separations, the (b)–(d) on the right-side of the figure show the spin-resolved conductances as functions of the bias voltage at three different separations R. The two strongly asymmetric Fano–Kondo resonances in panel (b) ($R=0$) become less pronounced as R increases; moreover, the splitting between $G^{\uparrow}$ and $G^{\downarrow}$ is reduced. As R increases, therefore, the resulting polarization loses its structure and approaches a constant. We note that Ref. [22], which studied an unpolarized tip, reported a similar R dependence of the Fano–Kondo line shape: a Fano antiresonance for $R \approx 0$, a less pronounced antiresonance for intermediate R and an approximately flat profile (background) for large R, a trend analogous to the evolution of the solid and dashed curves in panels (b)–(d). Due to the ferromagnetism of the tip, however, $G^{\uparrow}$ is dominant over $G^{\downarrow}$; the resulting polarization $\wp$ thus approaches the background polarization p.

5. Conclusions

We studied theoretically the spin-resolved conductance for a ferromagnetic STM tip coupled to an adatom on a nonmagnetic metallic host. For each spin component, the spin-resolved conductance displays a Fano antiresonance. The ferromagnetic polarization nonetheless tends to shift the two antiresonances to different energies. A window of bias voltages arises in which $G^{\downarrow} \approx 0$, while $G^{\uparrow}$ is maximum. In that window, the spin polarization $\wp$ remains close to unity. The application of an appropriately tuned bias voltage can therefore produce fully spin polarized currents. A ferromagnetic STM tip therefore constitutes a tunable spin polarizer.

Acknowledgments

We thank L.N. Oliveira for revising the text of the final version and M. Yoshida for fruitful discussions. This work was supported by the Brazilian agencies IBEM, CAPES, FAPESPA, and FAPERJ.

References

[1] A.C. Hewson, The Kondo Problem to Heavy Fermions, Cambridge University Press, Cambridge, 1993.
[2] U. Meirav, M.A. Kastner, S.J. Wind, Phys. Rev. Lett. 65 (1990) 771.
[3] D.G. Gordon, H. Shtrikman, D. Mahalu, D.A. Magder, U. Meirav, M.A. Kastner, Nature 391 (1998) 156.
[4] S.M. Cronenwett, T.H. Oosterkamp, L.P. Kouwenhoven, Science 281 (1998) 540.
[5] M. Sato, H. Aikawa, K. Kobayashi, S. Katsumoto, Y. Iye, Phys. Rev. Lett. 95 (2005) 066801.
[6] S. Hershfield, J.H. Davies, J.W. Wilkins, Phys. Rev. Lett. 67 (1991) 3720.
[7] S. Hershfield, J.H. Davies, J.W. Wilkins, Phys. Rev. B 46 (1992) 7046.
[8] Y. Meir, N.S. Wingreen, P.A. Lee, Phys. Rev. Lett. 70 (1993) 2601.
[9] N.S. Wingreen, Y. Meir, Phys. Rev. B 49 (1994) 11040.
[10] J. König, H. Shoeller, G. Schön, Phys. Rev. Lett. 76 (1996) 1715.
[11] J. König, J. Schmid, H. Shoeller, G. Schön, Phys. Rev. B 54 (1996) 16820.
[12] F. Simmel, R.H. Blick, J.P. Kotthaus, W. Wegscheider, M. Bichler, Phys. Rev. Lett. 83 (1999) 804.
[13] M. Krawiec, K.I. Wysokiński, Phys. Rev. B 66 (2002) 165408.
[14] J. Martinek, Y. Utsumi, H. Imamura, J. Barnaś, S. Maekawa, J. König, G. Schön, Phys. Rev. Lett. 91 (2003) 127203.
[15] J. Martinek, M. Sindel, L. Borda, J. Barnaś, J. König, G. Schön, J. von Delft, Phys. Rev. Lett. 91 (2003) 247202.
[16] M.-S. Choi, D. Sánchez, R. López, Phys. Rev. Lett. 92 (2004) 056601.
[17] Y. Utsumi, J. Martinek, G. Schön, H. Imamura, S. Maekawa, Phys. Rev. B 71 (2005) 245116.
[18] R. Świrkowicz, M. Wilczyński, M. Wawrzyniak, J. Barnaś, Phys. Rev. B 73 (2006) 193312.
[19] A.N. Pasupathy, R.C. Bialczak, J. Martinek, J.E. Grose, L.A.K. Donev, P.L. McEuen, D.C. Ralph, Science 306 (2004) 86.

[20] K. Hamaya, M. Kitabatake, K. Shibata, M. Jung, M. Kawamura, K. Hirakawa, T. Machida, T. Taniyama, Appl. Phys. Lett. 91 (2007) 232105.
[21] U. Fano, Phys. Rev. 124 (1961) 1866.
[22] V. Madhavan, W. Chen, T. Jamneala, M.F. Crommie, N.S. Wingreen, Science 280 (1998) 567.
[23] N. Knorr, M. Alexander Schneider, L. Diekhöner, P. Wahl, K. Kern, Phys. Rev. Lett. 88 (2002) 096804.
[24] K. Nagaoka, T. Jamneala, M. Grobis, M.F. Crommie, Phys. Rev. Lett. 88 (2002) 077205.
[25] P. Wahl, L. Diekhöner, G. Wittich, L. Vitali, M.A. Scheneider, K. Kern, Phys. Rev. Lett. 95 (2005) 166601.
[26] Y.-S. Fu, S.-H. Ji, X. Chen, X.-C. Ma, R. Wu, C.-C. Wang, W.-H. Duan, X.-H. Qiu, B. Sun, P. Zhang, J.-F. Jia, Q.-K. Xue, Phys. Rev. Lett. 99 (2007) 256601.
[27] A. Schiller, S. Hershfield, Phys. Rev. B 61 (2000) 9036.
[28] O. Újsághy, J. Kroha, L. Szunyogh, A. Zawadowski, Phys. Rev. Lett. 85 (2000) 2557.
[29] M. Plihal, J.W. Gadzuk, Phys. Rev. B 63 (2001) 085404.
[30] V. Madhavan, W. Chen, T. Jamneala, M.F. Crommie, N.S. Wingreen, Phys. Rev. B 64 (2001) 165412.
[31] S. Heinze, M. Bode, A. Kubetzka, O. Pietzsch, X. Nie, S. Blügel, R. Wiesendanger, Science 288 (2000) 1805.
[32] I. Zutic, J. Fabian, S. Das Sarma, Rev. Mod. Phys. 76 (2004) 323.
[33] K.R. Patton, S. Kettemann, A. Zhuravlev, A. Lichtenstein, Phys. Rev. B 76 (2007) 100408(R).
[34] A.C. Seridonio, F.M. Souza, I.A. Shelykh, J. Phys. Condens. Matter 21 (2009) 95003.
[35] S. Doniach, M. Sunjic, J. Phys. C 3 (1970) 285.
[36] H.O. Frota, L.N. Oliveira, Phys. Rev. B 33 (1986) 7871.
[37] H.O. Frota, Phys. Rev. B 45 (1992) 1096.
[38] The Doniach–Sunjic formula was recently used to fit experimental Kondo resonances, revealing a quite good agreement. See Ref. [26].
[39] An alternative spin filter based on Fano effect was proposed by for the T-Shaped QD system in the zero-bias limit, see M.E. Torio, K. Hallberg, S. Flach, A.E. Miroshnichenko, M. Titov, Eur. Phys. J. B 37 (2004) 399. See also Ref. [40].
[40] A.C. Seridonio, M. Yoshida, L.N. Oliveira, arXiv:cond-mat/0701529, 2008.
[41] P.W. Anderson, Phys. Rev. 124 (1961) 41.
[42] T.A. Costi, A.C. Hewson, V. Zlatić, J. Phys. Condens. Matter 6 (1994) 2519.
[43] J.C. Egues, Phys. Rev. Lett. 80 (1998) 4578.
[44] M. Popp, D. Frustaglia, K. Richter, Nanotechnology 14 (2003) 347.
[45] A.A. Kiselev, K.W. Kim, J. Appl. Phys. 94 (2003) 4001.
[46] I.A. Shelykh, N.G. Galkin, N.T. Bagraev, Phys. Rev. B 72 (2005) 235316.
[47] F.M. Souza, J.C. Egues, A.P. Jauho, Phys. Rev. B 75 (2007) 165303.
[48] C.A. Merchant, N. Marković, Phys. Rev. Lett. 100 (2008) 156601.
[49] F.M. Souza, Phys. Rev. B 76 (2007) 205315.
[50] F.M. Souza, J.A. Gomez, Phys. Stat. Sol. b 246 (2009) 431.